Journal of Visualized Experiments
Blood flow imaging with Ultrafast Doppler
--Manuscript Draft--

Article Type:	Invited Methods Collection - JoVE Produced Video
Manuscript Number:	JoVE61838R1
Full Title:	Blood flow imaging with Ultrafast Doppler
Corresponding Author:	Olivier Villemain Hospital for Sick Children Toronto, Ontario CANADA
Corresponding Author's Institution:	Hospital for Sick Children
Corresponding Author E-Mail:	olivier.villemain@sickkids.ca
Order of Authors:	Jerome Baranger
	Luc Mertens
	Olivier Villemain
Additional Information:	
Question	**Response**
Please indicate whether this article will be Standard Access or Open Access.	Standard Access (US$2,400)
Please indicate the **city, state/province, and country** where this article will be **filmed**. Please do not use abbreviations.	Toronto, Ontario, Canada
Please confirm that you have read and agree to the terms and conditions of the author license agreement that applies below:	I agree to the Author License Agreement
Please specify the section of the submitted manuscript.	Engineering
Please provide any comments to the journal here.	

1   **TITLE:**
2   Blood Flow Imaging with Ultrafast Doppler
3
4   **AUTHORS AND AFFILIATIONS:**
5   Jerome Baranger[1,2], Luc Mertens[1,2], Olivier Villemain[1,2,3]
6
7   [1]Translational Medicine Department, The Hospital for Sick Children, PGCRL Research Institute
8   [2]The Labatt Family Heart Centre, Department of Pediatric, The Hospital for Sick Children,
9   University of Toronto, Toronto, Ontario, Canada.
10 [3]Medical Biophysics Department, University of Toronto, Toronto, Ontario, Canada
11
12 Email addresses of co-authors:
13 Jerome Baranger   (jerome.baranger@sickkids.ca)
14 Luc Mertens   (luc.mertens@sickkids.ca)
15 Olivier Villemain   (olivier.villemain@sickkids.ca)
16
17 **KEYWORDS:**
18 Ultrasound, ultrafast, medical imaging, blood flow, Doppler, high framerate, clutter filter, plane
19 wave, biomedical engineering
20
21 **SUMMARY:**
22 This protocol shows how to apply ultrafast ultrasound Doppler imaging to quantify blood flows.
23 After a 1 s long acquisition, the experimenter has access to a movie of the full field of view with
24 axial velocity values for each pixel every ≈0.3 ms (depending on the ultrasound time of flight).
25
26 **ABSTRACT:**
27 The pulsed-Doppler effect is the main technique used in clinical echography to assess blood flow.
28 Applied with conventional focused ultrasound Doppler modes, it has several limits. Firstly, a finely
29 tuned signal filtering operation is needed to distinguish blood flows from surrounding moving
30 tissues. Secondly, the operator must choose between localizing the blood flows or quantifying
31 them. In the last two decades, ultrasound imaging has undergone a paradigm shift with the
32 emergence of ultrafast ultrasound using unfocused waves. In addition to a hundredfold increase
33 in framerate (up to 10000 Hz), this new technique also breaks the conventional
34 quantification/localization trade-off, offering a complete blood flow mapping of the field of view
35 and a simultaneous access to fine velocities measurements at the single-pixel level (down to 50
36 µm). This data continuity in both spatial and temporal dimensions strongly improves the
37 tissue/blood filtering process, which results in an increase sensitivity to small blood flow
38 velocities (down to 1 mm/s). In this method paper, we aim to introduce the concept of ultrafast
39 Doppler as well as its main parameters. Firstly, we summarize the physical principles of unfocused
40 wave imaging. Then, we present the Doppler signal processing main steps. Particularly, we
41 explain the practical implementation of the critical tissue/blood flow separation algorithms and
42 on the extraction of velocities from these filtered data. This theoretical description is
43 supplemented by in vitro experiences. A tissue phantom embedding a canal with flowing blood-
44 mimicking fluid is imaged with a research programmable ultrasound system. A blood flow image

45   is obtained and the flow characteristics are displayed for several pixels in the canal. Finally, a
46   review of in vivo applications is proposed, showing examples in several organs such as carotids,
47   kidney, thyroid, brain and heart.
48
49   **INTRODUCTION:**
50   Ultrasound imaging is one of the most commonly used imaging techniques in clinical practice and
51   research activities. The combination of ultrasound wave emission in the biological tissues
52   followed by the recording of the backscattered echoes allows the reconstruction of anatomical
53   images, the so-called "B-Mode". This method is perfectly adapted for soft tissue imaging, such as
54   biological tissues, which typically permit the penetration of ultrasound over several centimeters,
55   with a propagation speed of ≈1540 m/s. Depending on the center frequency of the ultrasound
56   probe, images with a resolution from 30 μm to 1 mm are obtained. Furthermore, it is well known
57   that the motion of an acoustic source, affects the physical characteristics of the associated waves.
58   Particularly, the link between the frequency shifts of a wave relative to the speed of its source is
59   described as the Doppler effect[1], whose simplest manifestation is the changing siren's pitch of a
60   moving ambulance. Ultrasound imaging has long used this physical effect to observe the moving
61   red blood cells[2], and it proposes a variety of imaging modes commonly labelled "Doppler
62   imaging". These modes enable the assessment of blood flows in very different applications and
63   organs, such as brain, heart, kidney or peripheral arteries.
64
65   Remarkably, most of the currently available ultrasound systems rely on the same technology,
66   referred to as conventional ultrasound. The underlying principles are the following: an acoustic
67   beam insonifies the field of view and is swept along the ultrasound transducer aperture. For each
68   position of the beam, the echoes are recorded and converted into a line of the final image. By
69   progressively moving the beam along the transducer, the whole field of view can be imaged line-
70   per-line (**Figure 1**, left panel). This strategy was well adapted to the electrical constraints and
71   computing power prevailing until the beginning of the 21st century. Nonetheless, it has several
72   drawbacks. Among these, the final framerate is limited to a few hundred images per second by
73   the beam scanning process. In terms of blood flow, this relatively low framerate affects the
74   maximum flow velocities that can be detected, which is dictated by the sampling criteria of
75   Shannon-Nyquist[3]. Moreover, conventional Doppler must deal with a complex tradeoff. In order
76   to assess the blood flow velocity in a particular region of interest (ROI), several echoes coming
77   from that ROI have to be successively recorded. This implies that the ultrasound beam is
78   temporarily maintained in a fixed position. The longer the echo ensemble, the better the velocity
79   estimation will be for that ROI. However, to produce a complete image of the field of view, the
80   beam must scan the medium. Therefore, one can sense the conflict between these two
81   constraints: holding the beam to precisely assess the velocity along one line, or moving the beam
82   to produce an image. The different conventional Doppler modes (i.e., Color Doppler or Pulse
83   Wave Doppler) directly reflect this tradeoff. Typically, the Color Doppler produces a low-fidelity
84   flow map used for localizing the vessels[4], and the Pulse Wave Doppler is then used to accurately
85   quantify the flow in a previously identified vessel[5].
86
87   These two limitations (low framerate and localization/quantification tradeoff) are overcome with
88   very high-framerate emerging techniques. Among these, the synthetic aperture approach[6] or the

89   multiline transmit technique can be cited[7]. In this study, we focus on the so-called Ultrafast
90   ultrasound method. Introduced two decades ago[8–10], this method also relies on the
91   emission/reception of ultrasounds, but with a radically different pattern. Indeed, instead of using
92   a scanning focused beam, ultrafast imaging uses plane wave or diverging waves, which are able
93   to insonify the field of view with a single emission. Following that single emission, the associated
94   electronics is also able to receive and process the huge number of echoes originating from the
95   whole field of view. At the end, an image can be reconstructed from a single emission/reception
96   pattern[11] (**Figure 1**, right panel). These unfocused emissions can have a low signal to noise ratio
97   (SNR) due to the spread of the acoustical energy. This can be tackled by emitting several titled
98   plane-waves (or diverging waves with different sources) and by adding the resulting images. This
99   method is named "coherent compounding"[12]. Two major consequences arise. Firstly, the
100 framerate only depends on the ultrasound time of flight and can reach typical values from 1 to
101 10 kHz. Secondly, this ensures the data continuity in both spatial and temporal dimensions, also
102 referred to as spatiotemporal coherence. The conventional localization/quantification tradeoff is
103 thus broken. This combination of a high framerate and spatiotemporal coherence has a
104 tremendous impact on the ability to detect blood flows with ultrasound. As compared to
105 conventional ultrasound, ultrafast ultrasound provides full characterization of the blood flow[3].
106 Practically, the user has access to the velocity time course in every pixel of the image, for the
107 whole duration of the acquisition (typically ≈1 s), with a timescale given by the framerate
108 (typically, a framerate of 5 kHz for a temporal resolution of 200 µs). This high framerate makes
109 the method suitable for a wide range of application such as fast flow in moving organs like heart
110 chambers[13] or myocardium with the coronary micro-perfusion[14]. Furthermore, it has been shown
111 that its spatiotemporal coherence strongly improves its ability to separate slow blood flow from
112 background moving tissues, therefore increasing the sensitivity to micro-vascular flow[15]. This
113 capacity gives access to the micro vasculature of the brain in both animals[16] and humans[17].
114
115 Hence, ultrafast ultrasound is well suited to image blood flow in a variety of situations. It is
116 restricted to soft biological tissues and will be strongly affected by the presence of hard interfaces
117 such as bones, or gas cavity such as the lung. The tuning of the physical parameters of the
118 ultrasound sequence allows the study of both slow (down to 1 mm/s[11,16]) and fast flows (up to
119 several m/s). A tradeoff exists between the spatial resolution and the depth of penetration.
120 Typically, a resolution of 50 µm can be achieved at the cost of a penetration around 5 mm.
121 Conversely, the penetration can be extended to 15-20 cm at the cost of a resolution of 1 mm. It
122 is worth noting that most ultrafast scanners such as the one used in this article only provide 2D
123 images.
124
125 Here, we propose a simple protocol to introduce the concept of Ultrafast Doppler imaging, using
126 a programmable research ultrasound scanner and Doppler phantom mimicking a vessel (artery
127 or vein) embedded in biological tissue.
128
129 **PROTOCOL:**
130
131 **1.   Doppler phantom preparation setup (Figure 2A)**
132

133   1.1.   Connect the peristaltic pump, the blood mimicking fluid reservoir, the pulse dampener
134   and the Doppler flow phantom with the plastic tubes.

135
136   1.2.   Choose the canal with a 4 mm diameter.

137
138   1.3.   Program the pump to eject 720 mL/min of fluid for 0.3 s and then to eject 50 mL/min for
139   0.7 s to respectively mimic the systole and diastole cardiac phases

140
141   1.4.   Run the pump and gently shake the pipes to expel potential air bubbles.

142
143   NOTE: The operator can choose a different canal diameter and different pump rate but will have
144   to ensure that the ultrasound sequence is fast enough to acquire the fastest flow velocities. Eq.
145   3 presented later can help to design the sequence.

146
147   **2.   Ultrafast ultrasound scanner setup (Figure 2A)**

148
149   2.1.   Connect the ultrafast-enabled research scanner to the host computer with the PCI
150   express link.

151
152   2.2.   Change the transducer adapter on the ultrasound scanner to match the probe connector,
153   then connect the probe.

154
155   2.3.   Run Matlab and activate the ultrasound scanner license.

156
157   NOTE: This section and the following implicitly assume the use of a Verasonics Vantage system.

158
159   **3.   Ultrasound sequence programming**

160
161   3.1.   Using the examples scripts, design a conventional focused "B-Mode" (i.e., echography)
162   sequence that will be used for probe positioning.

163
164   3.1.1. Set the imaging depth to 50 mm.

165
166   3.1.2. Set the focal depth to 35 mm.

167
168   3.2.   Using the examples scripts, design an ultrafast ultrasound sequence.

169
170   3.2.1. Set the imaging depth to 50 mm.

171
172   3.2.2. Program 3 tilted plane-waves at [-3,0,3] degree.

173
174   3.2.3. Set the pulse repetition frequency (PRF) to 12 kHz.

175
176   3.2.4. Use 4 half-cycles for the ultrasound waveform, with a center frequency depending on the

177   probe used. A center frequency of 5.2 MHz is assumed here.

178

179   3.2.5. Set the total duration to 1 s.

180

181   **4.**   **Probe positioning and data acquisition**

182

183   4.1.   Apply ultrasound gel on the probe's lens.

184

185   4.2.   Place the probe on the phantom and launch the B-Mode ultrasound sequence.

186

187   4.3.   Locate the canal of interest. The fluid appears darker than the surrounding tissue. Place
188   the probe in longitudinal view.

189

190   4.4.   Manually maintain the probe in the position of interest.

191

192   4.5.   End the B-Mode sequence and launch the ultrafast sequence acquisition script.

193

194   **5.**   **Image reconstruction (Figure 2B)**

195

196   5.1.   Once the sequence is over, save the raw data (also called Radio-Frequency data, "RF").

197

198   5.2.   Launch the image reconstruction script using the ultrasound system default software. At
199   the end of the process, the IQ data matrix should be created.

200

201   NOTE: The ultrasound echoes are recorded on each element of the probe and for each
202   emission/reception, then stored in the RF data matrix. The image reconstruction applied the
203   appropriate delay law to each channel and results in the so-called "IQ" (In-Phase/Quadrature)
204   matrix. The complex IQ matrix has three dimensions: two for space (image depth and width) and
205   one for time

206

207   **6.**   **Clutter filtering (Figure 2C)**

208

209   NOTE: For steps 6-7, see the Matlab script provided in the **Supplementary Material**.

210

211   6.1.   Reshape the 3D (space x space x time) IQ matrix into a 2D (space x time) Casorati matrix,
212   named IQr.

213

214   6.2.   Compute the singular value decomposition[15] of IQr (Eq. 1).

$$[U, S, V] = svd(IQr)$$ Eq. 1

215   6.3.   Compute the Spatial Similarity Matrix C using the spatial singular vectors U as described
216   by Baranger et al.[18] (II, D), and identify the blood subspace boundaries N.

217

218   6.4.   Use this cutoff N to filter the IQ data as described in Demene et al.[15] (II,C).

219
220 **7.   Flow visualization and velocity measurements (Figure 2C)**
221
222 7.1.   Compute power Doppler map PD by integrating the envelope of the filtered data
223 IQ_f along the temporal dimension (Eq. 2). The 3D coordinates z, x and t are respectively the
224 depth, width and temporal dimension, and n_t is the number of frames acquired.

$$PD(z,x) = \frac{1}{n_t}\sum_{t=1}^{n_t}\left|IQ_f(z,x,t)\right|^2 \qquad\qquad \text{Eq. 2}$$

225
226 7.2.   Display the PD map in logarithm scale. To set the dynamic range, compute the mean PD
227 in a region outside the canal and use this value in dB as the lower bound of the dynamic range. A
228 typical dynamic range is [-30, 0] dB.
229
230 7.3.   Define a circular region of interest (ROI) on the image, containing 1 to 30 pixels.
231
232 7.4.   Average the IQ_f signal over the pixels of that ROI, to obtain a vector $IQ_f^{\overline{ROI}}$ of n_t time
233 points.
234 7.5.   Compute and display the Doppler spectrogram of $IQ_f^{\overline{ROI}}$, using the square magnitude of
235 the Short-Time Fourier Transform (STFT).
236
237 7.5.1. Set the STFT window to a 60-samples Hann window.
238
239 7.5.2. Set the STFT overlap to 90% of the window length.
240
241 7.6.   Overlay the center frequency at each time point of the spectrogram.
242
243 7.7.   Convert the frequency f values into blood axial velocities v_z using the Doppler formula
244 (Eq. 3). c_0 is the speed of sound in the medium and f_{TW} the center frequency of the transmitted
245 ultrasound waveform (here 5.2 MHz).

$$v_z = \frac{c_0\,f}{2\,f_{TW}} \qquad\qquad \text{Eq. 3}$$

246
247 **REPRESENTATIVE RESULTS:**
248 The quality of the acquisition and the post-processing is firstly assessed by visual inspection. The
249 shape of the canal must be clearly visible in the power Doppler image, and the tissue area must
250 appear dark. If the power Doppler signal is not restricted to the canal, it can mean that either the
251 clutter filter step went wrong (SVD threshold is too low), or the probe experienced a strong
252 movement during the acquisition.
253
254 After visual inspection, the study of the spectrogram inside the canal can provide good
255 information on the success or failure of the experiment. The spectrogram should be one-sided
256 (all the values above or below zeros). If the spectrogram is two-sided, aliasing is present. In that

257 case, either the flow is too fast, or the PRF is too low.
258
259 If these quality criteria are met, the blood velocities can be extracted from any ROI in the image
260 (**Figure 2C**). Tuning the size of the ROI allows more or less averaging of the signals. The velocity
261 time course of a given ROI can then be used for multiple analysis such as the computation of
262 resistivity indexes[19], wall shear stress estimation[20], reactive hyperemia quantification[14] and much
263 more[21][22].
264
265 **Figure 3A-D** shows the transposition of this protocol to various in vivo applications. In particular,
266 the neonate brain acquisition (**Figure 3B**) exhibits vessels with very different flow characteristics,
267 from small cortical venules and arterioles to the major pericallosal artery. **Figure 3D** illustrates
268 the ability of ultrafast Doppler to extract blood flow signal in a strongly moving organ such as the
269 myocardium.
270
271 **FIGURE AND TABLE LEGENDS:**
272
273 **Figure 1**: **Conventional and Ultrafast Ultrasound Imaging.** Legend: **(Left)** Conventional imaging
274 with focused emission. **(Right)** Ultrafast imaging with plane wave emission. (adapted from
275 Villemain et al.[22]).
276
277 **Figure 2: Ultrafast Doppler protocol workflow.** (**A**) Experimental setup including the ultrafast-
278 enabled scanner and the Doppler flow phantom. The dashed rectangle on the phantom indicates
279 the footprint of the ultrasound transducer. (**B**) Automated data acquisition chain and post-
280 processing triggered by a simple user button-press. (**C**) (Top) Extraction of blood flow signal and
281 suppression of the tissue background noise ("clutter filter") and display of the blood spectrogram
282 in any ROI of the field of view. (Bottom) Spectrogram showing the blood velocity distribution in
283 the ROI at different time points. The mean velocity in the ROI is traced in dashed green.
284
285 **Figure 3: Power Doppler images.** Ultrafast Doppler acquisitions on several organs. (**A**) Adult
286 transplanted kidney, (**B**) Sagittal view of a human neonate brain, (**C**) Adult thyroid, (**D**) Intramural
287 coronary vasculature in open-chest swine experiments, (**E**) 3D directional power Doppler of the
288 carotid artery and the jugular vein of a healthy volunteer (blue = descending flow, red = ascending
289 flow). Several spectrograms are extracted for different ROI. (**A-C** are adapted from Baranger et
290 al.[18], **D** is adapted from Maresca et al.[14], **E** is adapted from Provost et al.[23]). For each acquisition,
291 the center frequency, number of angles, PRF and maximum depth was tuned according to the
292 situation. The dynamic range for panel **A, B** and **C** are respectively -27, -35 and -30 dB. It was not
293 provided for panel D and E.
294
295 **DISCUSSION:**
296 Several variations are possible around the main frame of this protocol.
297
298 **Hardware concerns**
299 If the user supplies its custom host computer, the motherboard and the computer's case must
300 have an available PCI express slot. The CPU must also have enough PCIe lanes to handle all the

301 devices.
302
Probe selection
304 The ultrasound probe (also named transducer) is chosen according to the spatial resolution
305 needed and to the geometry of the field of view. The higher the center frequency of the probe,
306 the better the spatial resolution but the shorter the imaging depth. Linear, curved or phased-
307 array probes provide field of view of respectively rectangular, circular sector and flat-top sector
308 shapes.
309
Angle dependency
311 Ultrafast Doppler shares the same constraint as conventional Doppler regarding the dependency
312 to the blood flow angle. Indeed, the underlying Doppler effect only allows the detection of
313 movement in the axial direction, meaning toward the probe surface, or away from the probe.
314 Hence, only the axial components of the blood scatterers velocity vectors are actually measured.
315 The true velocity can be recovered by manually indicating the local angle of the blood flow with
316 the vertical axis, but this angle cannot always be correctly assessed. In an extreme case where
317 the flow is perfectly orthogonal to the vertical depth axis, the Doppler effect cannot be used to
318 reliably measure the blood velocity. More advanced techniques can measure multiple
319 projections of the velocity vectors on several axes and can ultimately reconstruct the true velocity
320 vector. These angle independent approaches are referred to as vector flow imaging[8–10, 24].
321
Aliasing
323 The protocol described in this manuscript has several limitations. Firstly, the Shannon-Nyquist
324 sampling theorem states that the maximum measurable frequency in the sampled signal cannot
325 exceed half of the framerate. With 3 angles and a PRF of 12 kHz, the framerate is 4 kHz.
326 Consequently, we can derive from Eq. 3 that the maximum detectable axial velocity is 30 cm/s.
327 Considering the angle of the canal in the phantom, this framerate allows the detection of flow
328 with velocities up to 96 cm/s. Velocities above this threshold will appear aliased in the Doppler
329 spectrogram. For the presented setup, the peak velocities were ranging between 95 cm and 8
330 cm/s.
331
Clutter filter optimization
333 Blood flow visualization strongly relies on the ability to separate the blood signals from the slowly
334 moving tissue background. Depending on the respiration or the sonographer's hand motion, the
335 tissue can move with speeds similar to slow blood flow. Therefore, the so-called "clutter filter"
336 stage aims to cancel tissue signals. The ability to detect slow blood flows only relies on the
337 efficiency of this clutter filter stage. It has been shown that leveraging the spatiotemporal
338 coherence of ultrafast ultrasound strongly increases the outcome of these filters. The singular
339 value decomposition filter described by Demene et al.[15] is widely used. Optimization of that
340 method[18] or more complex algorithms such as high-order SVD[25], principal component pursuit[26],
341 independent component analysis[27] or other low-rank decomposition[28] can improve the quality
342 of the filtered data. It is worth mentioning that in the presented in vitro setup, the only source of
343 clutter is the hand motion of the operator. In vivo, many other factors such as respiration and
344 arterial pulsatility are likely to induce clutter that is more predominant. In these cases, the

345 advanced SVD filter described in this protocol becomes of prime importance.
346

Spectrogram interpretation

Spectrograms are the most common tool to study blood flow characteristics in both conventional and ultrafast Doppler ultrasound. For each time point, the spectrogram shows in grayscale the velocity distribution inside the considered ROI. Complex flows such as non-laminar flows will hence naturally broaden this spectrum. However, this link between spectral broadening and velocity distribution is only true to a certain extent. It has been shown by several studies that the spectrogram width, also call spectral broadening, is indeed linked to the velocity distribution in the ROI but also to several geometrical parameters of the imaging system (array width, angles, etc)[29–31]. Therefore, while the spectrogram of a steady laminar and homogeneous flow should be a thin, flat line, it shows in practice a certain width that does not reflect the velocity distribution, but rather the geometry of the imaging setup. This potential pitfall can lead to incorrect velocity measurements. It is recommended to consider the mean velocity inside the ROI (**Figure 1C** dashed green line) to avoid these effects[32].

3D acquisitions

The present protocol was realized with a standard linear array transducer, resulting in 2D images. Nevertheless, 3D acquisitions can be performed, either by mechanically scanning the medium with a motorized linear probe[16], or by using row-column arrays[33] or matrix arrays[34]. The drawbacks to these new methods are the high computing costs and, for matrix probes, the need of specific scanners. An example of 3D acquisition is shown in **Figure 3E**.

Safety issues

Most of the research ultrafast ultrasound scanner are not approved for clinical use. It is the responsibility of the experimenter to comply with the standards prevailing in their country, both in term of electrical safety and acoustic output. For the latter, the FDA standards[35] and the IEC 62127-1 International Standard[36] must be considered.

Conclusion

In this paper, we have proposed a standard protocol to image blood flow with Ultrafast Doppler. By practicing on a calibrated flow phantom, the operator can eventually check the accuracy of their measurements. The protocol allows the user to design and execute an ultrafast ultrasound acquisition using plane-wave compounding. Ultimately, a post-processing framework is described and provides the first tool to display the blood flow profile in any region of interest of the image.
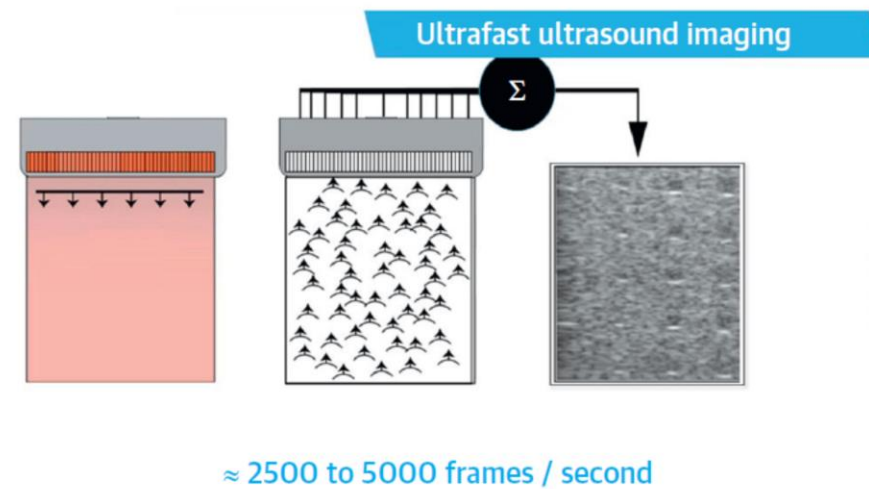
DISCLOSURES:
No conflict of interest

REFERENCES:
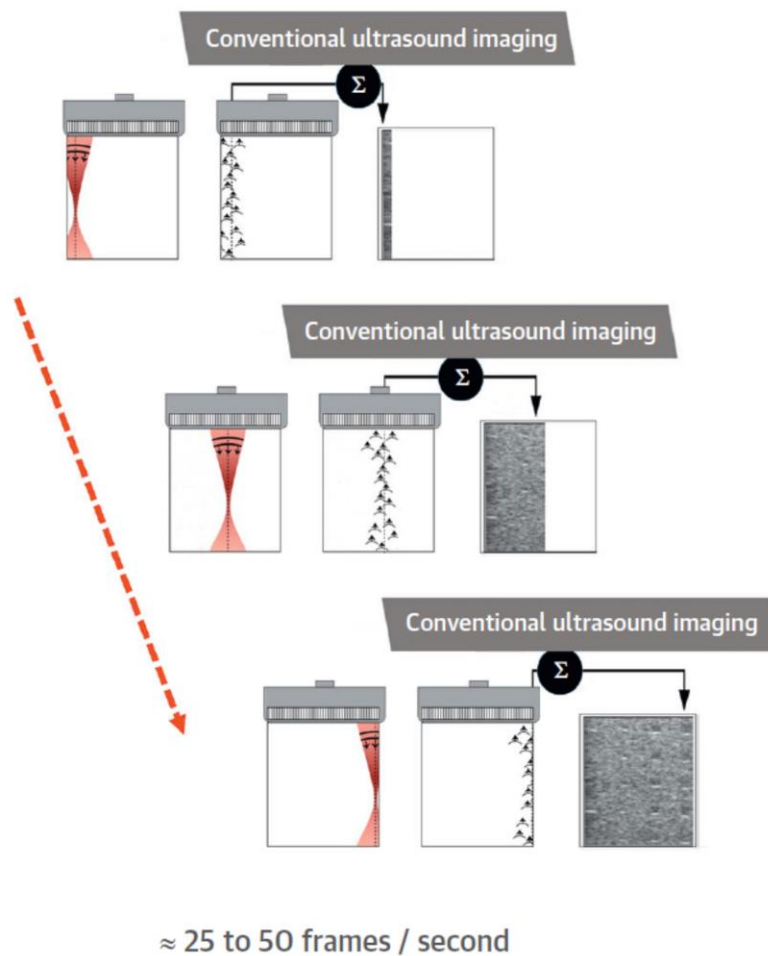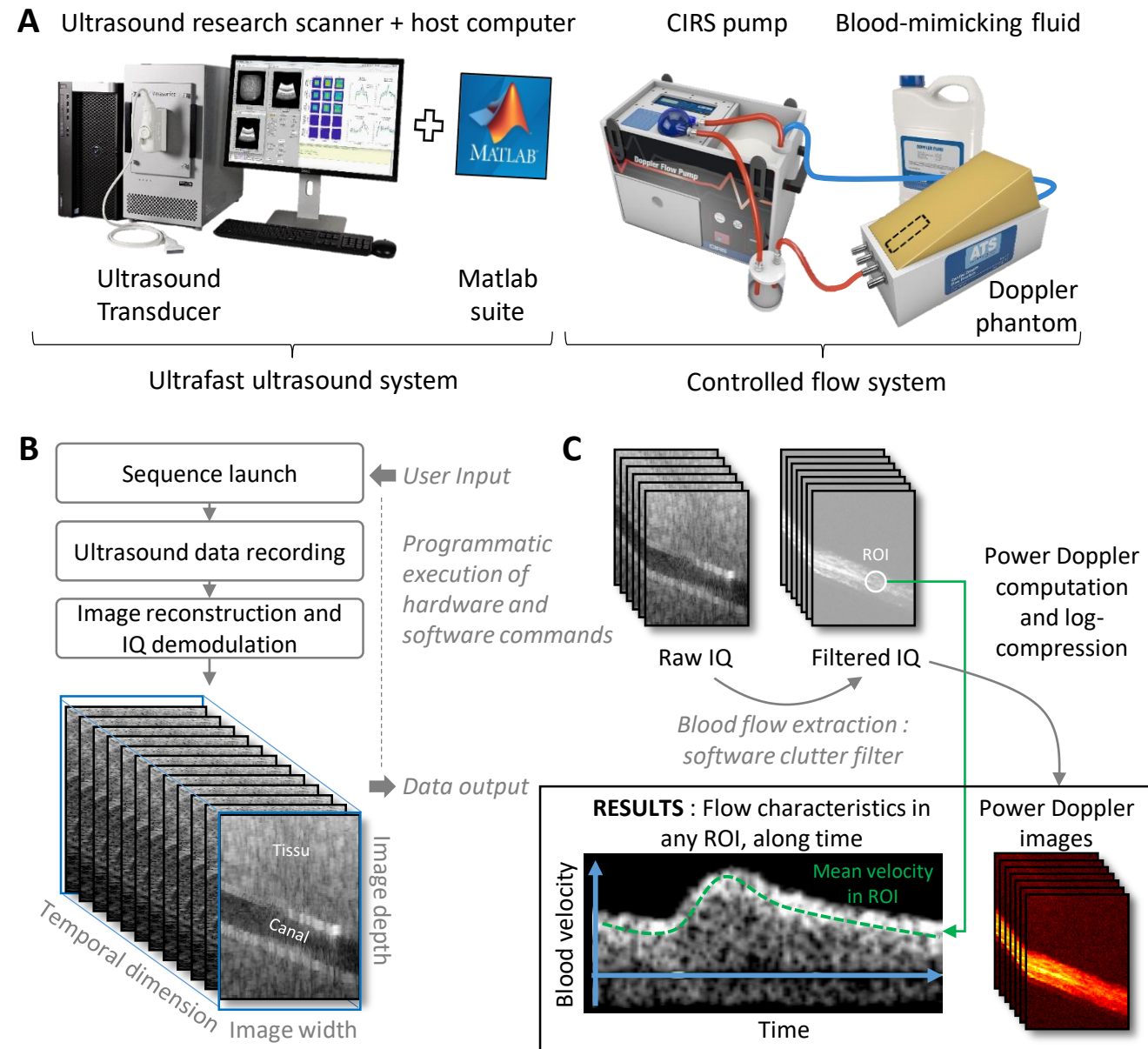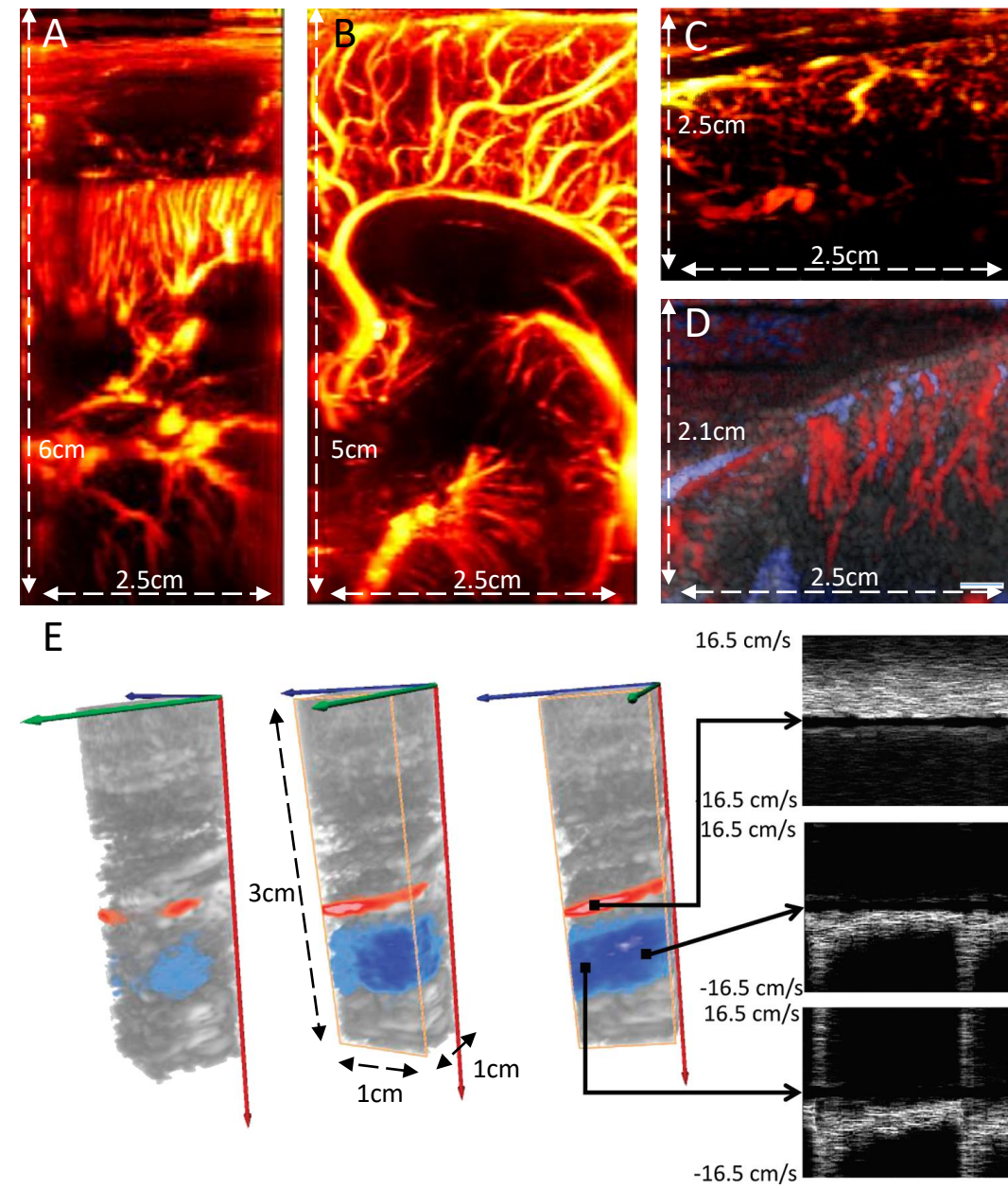
389   1.   Doppler, C. Ueber das farbige Licht der Doppelsterne und einiger anderer Gestirne des
390   Himmels.   at
391   <https://books.google.fr/books?hl=fr&lr=&id=mu9p8nmmSXgC&oi=fnd&pg=PA1&dq=Über+da
392   s+farbige+Licht+der+Doppelsterne+und+einiger+anderer+Gestirne+des+Himmels&ots=MDeLsX
393   4TLD&sig=cGmUuyNLfjWwNO9OUamlwdhP-s8#v=onepage&q=Über   das   farbige   Licht   der
394   Doppelsterne un>.
395   2.   Bonnefous, O., Pesqué, P. Time domain formulation of pulse-Doppler ultrasound and
396   blood velocity estimation by cross correlation. *Ultrasonic Imaging*. **8** (2), 73–85 (2004).
397   3.   Bercoff, J. et al. Ultrafast compound doppler imaging: Providing full blood flow
398   characterization. *IEEE Transactions on Ultrasonics, Ferroelectrics, and Frequency Control*. **58** (1),
399   134–147 (2011).
400   4.   Evans, D.H., Jensen, J.A., Nielsen, M.B. Ultrasonic colour Doppler imaging. *Interface Focus*.
401   **1** (4), 490–502 (2011).
402   5.   Nuffer, Z., Rupasov, A., Bekal, N., Murtha, J., Bhatt, S. Spectral Doppler ultrasound of
403   peripheral arteries: a pictorial review. *Clinical Imaging*. **46**, 91–97 (2017).
404   6.   Jensen, J.A., Nikolov, S.I., Gammelmark, K.L., Pedersen, M.H. Synthetic aperture
405   ultrasound imaging. *Ultrasonics*. **44** (SUPPL.) (2006).
406   7.   Tong, L., Ramalli, A., Jasaityte, R., Tortoli, P., D'Hooge, J. Multi-transmit beam forming for
407   fast cardiac imaging-experimental validation and in vivo application. *IEEE Transactions on
408   Medical Imaging*. **33** (6), 1205–1219 (2014).
409   8.   Tanter, M., Bercoff, J., Sandrin, L., Fink, M. Ultrafast compound imaging for 2-D motion
410   vector estimation: application to transient elastography. *IEEE Transactions on Ultrasonics,
411   Ferroelectrics and Frequency Control*. **49** (10), 1363–1374, (2002).
412   9.   Udesen, J. et al. High frame-rate blood vector velocity imaging using plane waves:
413   Simulations and preliminary experiments. *IEEE Transactions on Ultrasonics, Ferroelectrics, and
414   Frequency Control*. **55** (8), 1729–1743 (2008).
415   10.   Hansen, K.L., Udesen, J., Gran, F., Jensen, J.A., Bachmann Nielsen, M. In-vivo examples of
416   flow patterns with the fast vector velocity ultrasound method. *Ultraschall in der Medizin
417   (Stuttgart, Germany : 1980)*. **30** (5), 471–477 (2009).
418   11.   Tanter, M., Fink, M. Ultrafast imaging in biomedical ultrasound. *IEEE Transactions on
419   Ultrasonics, Ferroelectrics, and Frequency Control*. **61** (1), 102–119 (2014).
420   12.   Montaldo, G., Tanter, M., Bercoff, J., Benech, N., Fink, M. Coherent plane-wave
421   compounding for very high frame rate ultrasonography and transient elastography. *IEEE
422   Transactions on Ultrasonics, Ferroelectrics and Frequency Control*. **56** (3), 489–506 (2009).
423   13.   Papadacci, C., Pernot, M., Couade, M., Fink, M., Tanter, M. High-contrast ultrafast imaging
424   of the heart. *IEEE Transactions on Ultrasonics, Ferroelectrics, and Frequency Control*. **61** (2), 288–
425   301 (2014).
426   14.   Maresca, D. et al. Noninvasive Imaging of the Coronary Vasculature Using Ultrafast
427   Ultrasound. *JACC: Cardiovascular Imaging*. **11** (6), 798–808 (2018).
428   15.   Demené, C. et al. Spatiotemporal Clutter Filtering of Ultrafast Ultrasound Data Highly
429   Increases Doppler and fUltrasound Sensitivity. *IEEE Transactions on Medical Imaging*. **34** (11),
430   2271–2285 (2015).
431   16.   Demené, C. et al. 4D microvascular imaging based on ultrafast Doppler tomography.
432   *NeuroImage*. **127**, 472–483 (2016).

433   17.   Demené, C. et al. Ultrafast Doppler reveals the mapping of cerebral vascular resistivity in
434   neonates. *Journal of Cerebral Blood Flow and Metabolism*. **34** (6), 1009–1017 (2014).
435   18.   Baranger, J., Arnal, B., Perren, F., Baud, O., Tanter, M., Demene, C. Adaptive
436   Spatiotemporal SVD Clutter Filtering for Ultrafast Doppler Imaging Using Similarity of Spatial
437   Singular Vectors. *IEEE Transactions on Medical Imaging*. **37** (7), 1574–1586 (2018).
438   19.   Demené, C. et al. Ultrafast Doppler Reveals the Mapping of Cerebral Vascular Resistivity
439   in Neonates. *Journal of Cerebral Blood Flow & Metabolism*. **34** (6), 1009–1017 (2014).
440   20.   Goudot, G. et al. Wall Shear Stress Measurement by Ultrafast Vector Flow Imaging
441   for Atherosclerotic Carotid Stenosis. *Ultraschall in der Medizin - European Journal of Ultrasound*.
442   (2019).
443   21.   Demené, C., Mairesse, J., Baranger, J., Tanter, M., Baud, O. Ultrafast Doppler for neonatal
444   brain imaging. *NeuroImage*. **185**, 851–856 (2019).
445   22.   Villemain, O. et al. Ultrafast Ultrasound Imaging in Pediatric and Adult Cardiology. *JACC:*
446   *Cardiovascular Imaging*. (2019).
447   23.   Provost, J., Papadacci, C., Demene, C., Gennisson, J.L., Tanter, M., Pernot, M. 3-D ultrafast
448   doppler imaging applied to the noninvasive mapping of blood vessels in Vivo. *IEEE Transactions*
449   *on Ultrasonics, Ferroelectrics, and Frequency Control*. **62** (8), 1467–1472 (2015).
450   24.   Osmanski, B.F., Montaldo, G., Fink, M., Tanter, M. In vivo out-of-plane Doppler imaging
451   based on ultrafast plane wave imaging. *IEEE International Ultrasonics Symposium, IUS*. **62** (4), 76–
452   79 (2013).
453   25.   Kim, M.W., Zhu, Y., Hedhli, J., Dobrucki, L.W., Insana, M.F. Multi-dimensional Clutter Filter
454   Optimization for Ultrasonic Perfusion Imaging. *IEEE Transactions on Ultrasonics, Ferroelectrics,*
455   *and Frequency Control*. **65** (11), 2020–2029 (2018).
456   26.   Chau, G., Li, Y.L., Jakovljevic, M., Dahl, J., Rodr, P. Wall Clutter Removal in Doppler
457   Ultrasound using Principal Component Pursuit. (October) (2018).
458   27.   Tierney, J., Baker, J., Brown, D., Wilkes, D., Byram, B. Independent Component-Based
459   Spatiotemporal Clutter Filtering for Slow Flow Ultrasound. *IEEE Transactions on Medical Imaging*.
460   **PP** (c), 1–1 (2019).
461   28.   Zhang, N., Rivaz, H. Clutter Suppression in Ultrasound: Performance Evaluation and
462   Review of Low-Rank and Sparse Matrix Decomposition Methods. *BioMedical Engineering Online*.
463   **19**, 37 (2020).
464   29.   Guidi, G., Licciardello, C., Falteri, S. Intrinsic spectral broadening (ISB) in ultrasound
465   Doppler as a combination of transit time and local geometrical broadening. *Ultrasound in*
466   *Medicine and Biology*. **26** (5), 853–862 (2000).
467   30.   Cloutier, G., Shung, K.K., Durand, L.G. Experimental Evaluation of Intrinsic and
468   Nonstationary Ultrasonic Doppler Spectral Broadening in Steady and Pulsatile Flow Loop Models.
469   *IEEE Transactions on Ultrasonics, Ferroelectrics, and Frequency Control*. **40** (6), 786–795 (1993).
470   31.   Winkler, A.J., Wu, J. Correction of intrinsic spectral broadening errors in doppler peak
471   velocity measurements made with phased sector and linear array transducers. *Ultrasound in*
472   *Medicine and Biology*. **21** (8), 1029–1035 (1995).
473   32.   Osmanski, B.F., Bercoff, J., Montaldo, G., Loupas, T., Fink, M., Tanter, M. Cancellation of
474   Doppler intrinsic spectral broadening using ultrafast Doppler imaging. *IEEE Transactions on*
475   *Ultrasonics, Ferroelectrics, and Frequency Control*. **61** (8), 1396–1408 (2014).
476   33.   Sauvage, J. et al. A large aperture row column addressed probe for in vivo 4D ultrafast

doppler ultrasound imaging. *Physics in Medicine and Biology*. **63** (21) (2018).

34. Correia, M., Provost, J., Tanter, M., Pernot, M. 4D ultrafast ultrasound flow imaging: *in vivo* quantification of arterial volumetric flow rate in a single heartbeat. *Physics in Medicine and Biology*. **61** (23), L48–L61 (2016).

35. Center for Devices and Radiological Health. FDA Information for Manufacturers Seeking Marketing Clearance of Diagnostic Ultrasound Systems and Transducers. FDA-2017-D-5372 (2008).

36. 61851, I. *IEC 62127-1 - Measurement and characterization of medical ultrasonic fields up to 40 MHz. 61010-1 © Iec:2001* (2013).

Conventional ultrasound imaging

Conventional ultrasound imaging

Conventional ultrasound imaging

≈ 25 to 50 frames / second

Ultrafast ultrasound imaging

≈ 2500 to 5000 frames / second

Figure

A Ultrasound research scanner + host computer · CIRS pump · Blood-mimicking fluid

Ultrasound Transducer · Matlab suite · Doppler phantom

Ultrafast ultrasound system · Controlled flow system

B

Sequence launch ← *User Input*

Ultrasound data recording

Image reconstruction and IQ demodulation

Programmatic execution of hardware and software commands

→ *Data output*

Temporal dimension · Image depth · Image width · Tissu · Canal

C

Raw IQ · Filtered IQ · ROI

Blood flow extraction : software clutter filter

Power Doppler computation and log-compression

RESULTS : Flow characteristics in any ROI, along time

Mean velocity in ROI

Blood velocity · Time

Power Doppler images

Name of Material/ Equipment	Company	Catalog Number	Comments/Description
Blood-mimicking fluid	CIRS Inc, Norfolk, Virginia, USA	069DTF	
Doppler flow phantom	CIRS Inc, Norfolk, Virginia, USA	ATS523A	
Matlab	MathWorks, Natick, Massachusetts, United States		
Peristaltic pump / Doppler flow pump	CIRS Inc, Norfolk, Virginia, USA	769	Include tubings and pulse dampener
Transducer adpter	Verasonics, Kirkland, Washington, USA	UTA 408-GE	
Ultrafast ultrasound research scanner	Verasonics, Kirkland, Washington, USA	Vantage 256	
Ultrasound probe/transducer	GE Healthcare	GE 9L-D	

Blood flow imaging with Ultrafast Doppler – Response to the reviewers

We sincerely thank the reviewers for having accepted to evaluate this manuscript.

Reviewer #1

Minor Concerns

1. *The protocol described in manuscript is essentially available in numerous other publications.*

The reviewer is right. The described protocol has been already used in other publications. The goal of this paper is to provide as much practical details as possible, including a video, to reach a public of non-experts.

Reviewer #2

Major Concerns

No major concerns

Minor Concerns

1. *First, I recommend that you change the title to "Blood flow imaging with an ultrafast Doppler method"*

We understand the reviewer concern and we thank him for rising this important point. There are indeed several way to achieve very high framerate with ultrasound imaging. Other methods like synthetic aperture imaging or multiline transmit can also achieve very high framerate. However, we deliberately chose the term Ultrafast Doppler (with capital letter) to avoid the confusion with these methods. Indeed, Ultrafast Doppler explicitly refers to the technique that uses coherently compounded unfocused waves (plane or diverging waves). It is referred as such in several publications and in commercial devices such as Supersonic Imagine devices. As the outcome of these multiple high-framerate methods are different between each other, we think that the current title is more suited for the paper. We added a few sentence in the introduction (l86) to clarify this point.

Osmanski, B.-F. *et al*. Ultrafast Doppler Imaging of Blood Flow Dynamics in the Myocardium. *IEEE Transactions on Medical Imaging*. 31 (8), 1661–1668, doi: 10.1109/TMI.2012.2203316 (2012).

Demené, C. *et al.* Ultrafast Doppler Reveals the Mapping of Cerebral Vascular Resistivity in Neonates. *Journal of Cerebral Blood Flow & Metabolism*. 34 (6), 1009–1017, doi: 10.1038/jcbfm.2014.49 (2014).

Bercoff, J. *et al.* UltraFast Doppler. *Supersonic Imagine Whitepaper* (2011).

2. *It is named b-mode imaging and not echography (p1l51)*

The reviewer is right, we modified this term accordingly.

The citation was modified to reference to the original publication of Christian Doppler, in German (l57)

4. *You should reference the pioneers in fast flow imaging: Udesen et al (2008) High frame-rate blood vector velocity imaging using plane waves: Simulations and preliminary experiments; IEEE, and Hansen et al (2009) In-vivo Examples of Flow Patterns with The Fast Vector Velocity Ultrasound Method;Ultraschall.*

These important works were added to the text, we thank the reviewer for rising this (l89).

5. *You should mention that the method you propose is angle dependent (p2l112->). This should also be mentioned in the section of conventional Doppler, where other limitations already are listed such as frame rate (p2l100->).*

The reviewer is right, angle dependency is a shared limitation of ultrafast and conventional Doppler. We added a full section in the discussion to address this concern, introducing vector flow imaging as a potential solution (l299).

6. *You mention that the spectrogram can be broadened by several factor, but you are missing that flow complexity also can broaden the curve. Please add this info (p9l302).*

Indeed, the complexity of the flow such as turbulences will affect the spectral broadening. We added a sentence to clarify that point (see Spectrogram interpretation) (l339)

7. *I miss a conclusion of the paper. Also, I miss limitations of the setup.*

We added a conclusion as requested, we were not sure if the editor allow such sections. We added a couple of sections in the discussion (angle dependency, aliasing) and completed others (clutter filter) in a way to emphasize more the limitation of the setup. (l364)

8. *In fig 3 you give examples of different fast US techniques. I recommend that you omit these examples and instead give an in-vitro and in-vivo example obtained with the setup presented in this paper.*

The fig. 3 uses only Ultrafast Doppler to produces these images. The panel E showing 4D volume also uses Ultrafast Doppler. We wanted to illustrate the multiple *in vivo* applications of Ultrafast Doppler. However, we do agree with the reviewer that the presented results used different parameters for the ultrafast sequences (framerate, number of angles, frequency). We added an explanation in the fig 3 caption to clarify that point. We think that we should keep this figure as it present important and diverse *in vivo* results of Ultrafast Doppler.

Reviewer #3

Major Concerns:

1. *The authors do a nice job of providing context and relevant background information in the introduction. However, there are a few limits mentioned without citation or clarification. For example, the resolution limits are stated to be 30um to 1mm. Wouldn't these limits be different for different probes? Also, the authors state 1mm/s as the lower bound on blood velocity estimation. Is this theoretical for the parameters used in this work? Please include additional clarification or citations for these claims.*

The reviewer is right, the spatial resolution is dependent of the center frequency of the probe. We tried to convey this message by saying that the spatial resolution depend "on the ultrasound emission frequency" but this statement may be unclear and we modified it. Regarding the lower bound for blood velocity, it is not a theoretical parameter. Technically, the only limitation to slow blood flow detection is the clutter filter process. It has been reported in the literature that flow down to 1 mm/s could be detected. We added two citations (Demene et al, Tanter&Fink) to support this claim. Also, we added a note on this in the clutter filter optimization section, in the discussion. (l325)

2. *In step 4, users are told to secure the probe in the position of interest. This will ensure, for the most part, stationary tissue which will make clutter filtering trivial. The authors elaborate on the importance of tissue clutter filtering when tissue motion is present in the discussion, but I think it would be helpful to make it clear that the protocol does not account for this. Really, a simple FIR filter would probably suffice for the proposed experiment given that no spectral overlap is likely present. Please clarify these points in steps 4 and 6 of the protocol.*

The reviewer is right; this requirement can create some confusion. We modified the protocol (step 4.4) and now only ask the operator to hold the probe manually. In this case, the setup imitate more accurately an in-vivo acquisition. In this case, the natural hand motion will create spectral overlap, at least for the slow blood velocities and the advanced clutter filter becomes more relevant. As the idea is to provide tools for *in vivo* experiments, we wanted to insist on this important signal processing step. We added a few sentences in the clutter filter section to highlight the fact that *in vivo* clutter will probably be more predominant and we thank the reviewer for rising this point. (l331)

Minor Concerns:

1. *What is the reasoning for using a 4mm diameter canal? Any size canal could be used, right? Users would just need to compute the flow rate needed to achieve some velocity using Q=Av? If so, I think this could be stated in the protocol. Also, it would be helpful to provide the estimated peak velocities within the canal at the two time points given the flow rates in step 2.*

The reviewer is right. Any canal could be used. We added a note on this after step 1.4 . We asked to choose the 4mm canal for two reasons. Firstly, with the described ultrasound sequence and pump rates, a smaller canal would engender too high velocities. Secondly, a 4mm canal is died enough to have several pixel in the canal transverse axis, and so it is possible to observe the parabolic profile of the flow inside the canal, which is an interesting property. The peak velocities are not straightforward to define as the

pump+tube+phantom is compliant and thus dampen the pressure pulses. We added the measured velocities at the end of the new aliasing section (l319).

2. *I assume the two different flow rates are used to mimic systole and diastole - if so, please include that reasoning in the protocol.*

Indeed, the pulsatile flow is chosen to mimic a cardiac cycle. We thank the reviewer and included this in the protocol to clarify that point (step 1.3).

3. *In step 3, readers are directed to use the example scripts. I assume this is referring to the example scripts provided by Verasonics? It is unclear to me if this protocol is specific to Verasonics systems. If it is, please state that in steps 2 and 3. If it is not, please cross check other systems to confirm that example scripts are available and provide these other available systems.*

The reviewer is right; this protocol uses a Verasonics scanner and is design assuming that the user also has this device. The aim of the protocol is not to teach the programming of the Verasonics system, hence we encourage the use of already available example script from the manufacturer. Even though other ultrafast system exists (ULA-OP, SARUS, UARP, SonixTouch, VisualSonics F2, etc), they might not be compatible with the recommended GE9L-D probe, and their handling and programming fall over the scope of this manuscript. JOVE editorial policy requires that the brand and name of the different materials are not explicitly mentioned in the manuscript but in an attached table. However, we do agree with the reviewer that this is a key point, and we added a note in the manuscript on that. We will however comply with the editor's constraint, should they want to remove this note (l150).

4. *A typical dynamic range of 30dB is proposed in the protocol, but I think it would be helpful to at least suggest an alternative, more adaptive way of choosing the dynamic range since this can really affect visualization. For example, it could be suggested to scale to the mean of the background ROI pixels, or something along those lines.*

The reviewer is right; the dynamic range can affect the visualization. We chose a 30dB value as it is a classical value for *in vivo* ultrafast Doppler acquisition. But indeed, scaling with the mean background noise floor seems a good idea and we added it to the protocol (step 7.2).

5. *In Figure 2C, I assume the "Filtered IQ data" are prior to computing power. If so, please show an arrow from "Filtered IQ data" to an additional image that is a log compressed power Doppler image to help clarify those additional steps.*
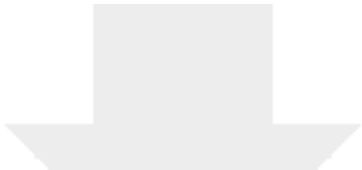
As suggested, we made the distinction between the power Doppler images (log compressed power Doppler) and the filtered IQ obtained after clutter filtering and used for spectral Doppler computation.

6. *Are all of the images in Figure 3 scaled to a 30dB dynamic range? Please indicate scaling in the caption.*

This information was indeed lacking. The dynamic range vary from on acquisition to the other, we added the value in the fig. 3 caption when they were provided in the original papers.

7. *In the "Probe Selection" section of the Discussion, the authors state that "the higher the center frequency of the probe, the higher the frequency but the shorter the imaging depth". Do you mean to say "the higher the center frequency of the probe, the better the resolution but the shorter the imaging depth"?*

We thank the reviewer for pointing out this mistake, and we apologize for it. This has been modified as suggested.

Click here to access/download

Supplemental Coding Files

JOVE_SupScript.m